

Observation of "Tamm States" in Superlattices

H. Ohno,^(a) E. E. Mendez, J. A. Brum,^(b) J. M. Hong, F. Agulló-Rueda,^(c) L. L. Chang, and L. Esaki
IBM Research Division, T. J. Watson Research Center, P.O. Box 218, Yorktown Heights, New York 10598

(Received 26 January 1990)

We have observed localized surface states (Tamm states) intentionally introduced in AlGaAs/GaAs superlattices by a terminating layer of AlAs. The formation of these states is manifested by excitonic interband transitions in photoluminescence excitation spectra. Critical confirmation is provided by photo-current experiments under an electric field that show additional transitions as well as anticrossing interactions between the Tamm states and the Stark-ladder states associated with the superlattice.

PACS numbers: 73.20.At, 73.20.Dx, 78.65.Fa

The assumption of a periodic potential with cyclic boundary conditions has proved very successful in explaining a large number of bulk properties of solids since the early days of solid-state physics. It was pointed out by Tamm¹ in 1932, however, that the inclusion of the neglected surface in a Kronig-Penney model results in electronic states localized at the surface of the solid under certain conditions. Although the field of surface science is one of the richest in physics, no experiments have been conducted to observe the surface state in the pure form that Tamm investigated theoretically. This is because the surfaces so far having been dealt with are real surfaces, where many effects are concurrently in operation, and because it has not been experimentally possible to construct and to engineer arbitrarily a model surface for a particular study. An example of this difficulty is provided by recent measurements of the surface electronic structure of CoSi₂(111), which have been unable to distinguish between a Tamm state and a surface resonance.²

In this Letter we report the first observation of the surface states discussed by Tamm, i.e., the Tamm states.³ We used AlGaAs/GaAs semiconductor superlattices, which allowed us to realize and manipulate a wide range of potential profiles. The experiments by optical spectroscopies made it possible to detect very sensitively the presence of such localized states. In addition, this work shows the ability and usefulness to create and study a prescribed "model surface" in a very controlled way in semiconductors.

The superlattice potential profile studied here is depicted schematically in Fig. 1(a). The present structure differs from typical superlattice structures in that one of the clad layers of AlGaAs [left-hand-side clad layer in Fig. 1(a)] is designed such that the corresponding barrier is ΔE higher than those in the rest of the superlattice, thus creating a "surface" barrier inside the semiconductor structure. This barrier is referred to as an internal surface hereafter.

In a superlattice, electron and hole minibands are formed in the conduction and valence bands, respectively, as a result of interwell coupling. A Tamm state appears when the barrier at the end is higher than the rest of the potential barriers in the superlattice. Here we

consider the case of only one Tamm state for simplicity: If barriers at both ends are raised, two Tamm states appear. This is illustrated in Fig. 1(a), where the nine electron eigenenergies of a nine-well Al_{0.2}Ga_{0.8}As/GaAs superlattice are plotted as a function of ΔE . For $\Delta E = 0$, all the states extend in the superlattice and their eigenenergies form a miniband. As ΔE increases, the highest-energy state starts to "peel off" from the miniband and its wave function starts to localize at the interface, whereas other wave functions stay delocalized and the width of the miniband remains essentially constant. The electron wave function of the highest eigenenergy is almost completely localized in the well at the internal surface when ΔE is 755 meV (which corresponds to an AlAs barrier), as shown in Fig. 1(b) together with the other eight wave functions. Because of the heavier mass, the heavy-hole Tamm state is even more localized.

The peculiar characteristics of the Tamm states make spectroscopic techniques very suitable for probing their presence in superlattices. Interband transitions between Tamm states should occur at higher energies than those

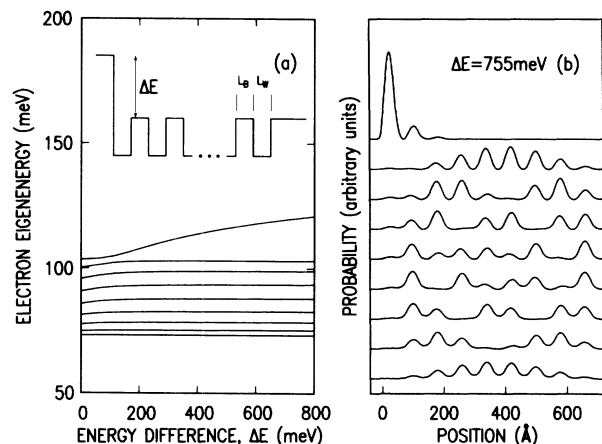


FIG. 1. (a) Electron eigenenergies of a nine-well Al_{0.2}Ga_{0.8}As/GaAs superlattice as a function of energy difference ΔE , defined in the inset, where the conduction-band profile of the superlattice is shown. $L_B = L_W = 40$ \AA . (b) Squared electron envelope function for $\Delta E = 755$ meV, shown in order of eigenenergy. The origin of the horizontal axis is at the left corner of the left-most well. Note the localized nature of the highest state.

between miniband states. In addition, since the electron and hole Tamm states are localized in the same well, we expect a higher exciton binding energy than that in the quasi-three-dimensional miniband states, which should give rise to a strong excitonic structure in the optical spectra. Moreover, in the presence of an electric field, the Tamm states are expected to behave differently due to their localized nature from the miniband states, which would experience a gradual Stark localization.⁴

The structures used in the present study were all grown by molecular-beam epitaxy on n^+ -type GaAs (001) substrates. From the substrate side, the undoped superlattice consists of 200-Å $\text{Al}_{0.2}\text{Ga}_{0.8}\text{As}$, nine GaAs wells ($L_W=40$ Å) separated by $\text{Al}_{0.2}\text{Ga}_{0.8}\text{As}$ barriers ($L_B=40$ Å), and 200-Å AlAs; this entire structure is repeated 3 times. The conduction-band profile of one of these units is identical to the one shown in Fig. 1(a). A $\sim 2\text{-}\mu\text{m}$ Si-doped n^+ -type GaAs ($n=2\times 10^{18}\text{ cm}^{-3}$) buffer layer was grown before the superlattice structures. On the superlattice, 500 Å of n^+ -type GaAs was grown to minimize the effect of the band bending associated with the real surface.

Photoluminescence (PL), photoluminescence excitation (PLE), and photocurrent (PC) spectra were measured at 5 K under excitation by a Kr^+ laser-pumped LD700 dye laser in the range of 1.60–1.72 eV. Electric fields up to 40 kV/cm were applied to the structure. A 100-Å of Au deposited on the surface and an In Ohmic contact at the backside of the sample were used to apply an electric field.

Figure 2 shows PL and PLE spectra at 0-V bias. One immediately notices a strong excitonic peak near 1.67 eV in addition to the well established electron-heavy-hole (HH) and electron-light-hole (LH) transitions. Included at the bottom of Fig. 2 are the calculated energies using the envelope-function approximation⁵ (EFA), for the HH, LH, and electron (Tamm)-heavy-hole (Tamm)

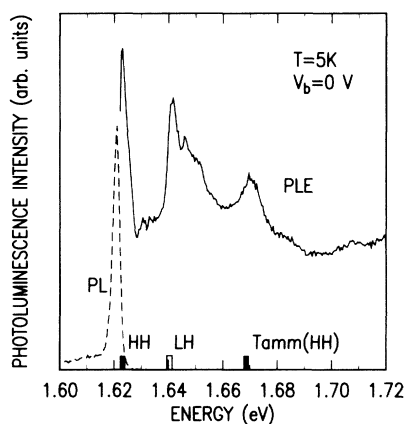


FIG. 2. PL and PLE spectra of a nine-well $\text{Al}_{0.2}\text{Ga}_{0.8}\text{As}/\text{GaAs}$ superlattice ($L_B=L_W=40$ Å) terminated by AlAs at one end to create an internal surface. Also shown are the excitonic transition energies calculated by the envelope-function approximation.

[labeled as Tamm (HH)] transitions. The separations of the excitonic peaks are in excellent agreement with the theoretical ones within ± 1 meV. Here, the GaAs band gap is assumed to be 1.519 eV and the exciton binding energies of 5 meV for HH and LH and 12 meV for Tamm (HH) transitions are used.⁶ The theoretical peaks are shifted rigidly by 7 meV to allow a direct comparison with the experiments. The possibility of the third transition being related to the excited states of the heavy-hole miniband is rejected since the transition is forbidden and cannot produce the sharp excitonic feature seen in Fig. 2. The assumed binding energies of HH and LH excitons are consistent with those estimated from the separations between the excitonic peaks and their corresponding continuum shoulders. The 5-meV binding energy is a consequence of the quasi-three-dimensional nature of the states in the minibands, as opposed to the value of 12 meV in quasi-two-dimensional excitonic transitions.⁶ The large binding of 12 meV, we believe, is responsible for the pronounced intensity of the Tamm (HH) structure in Fig. 2, in spite of the fact that the Tamm state is only one out of nine states.

The origin of the transitions becomes even clearer when they are measured under electric field and compared with EFA calculations. Figure 3 summarizes the energies of the features observed in PC spectra under various bias voltages, V_b . Solid circles are the transitions assigned to heavy-hole-related, open circles to light-hole-related, and open triangles are unidentified transi-

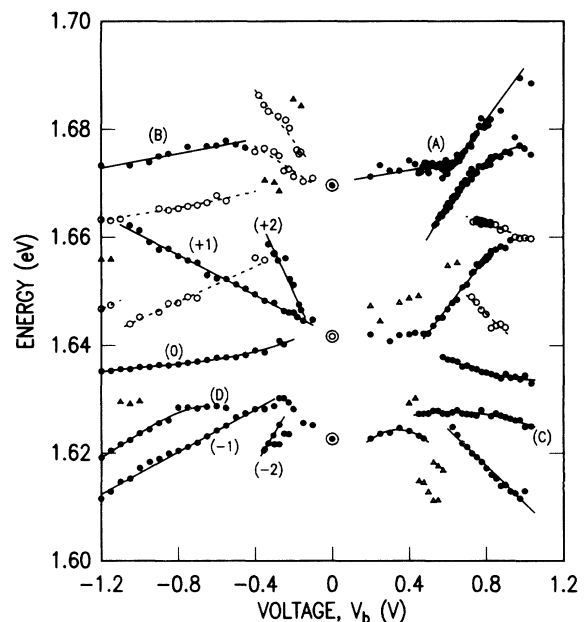


FIG. 3. Transition energies seen in PC spectra of the same sample used in Fig. 2 as a function of electric field. Solid circles are heavy-hole related and open circles are light-hole related. Open triangles are unidentified features. Concentric circles indicate the position of excitonic transitions seen in Fig. 2, where HH and Tamm (HH) are indicated with solid circles and LH with open circles.

tions. Concentric circles at 0 V indicate the positions of the excitonic transitions in the PLE spectra of Fig. 2. Positive polarity is defined as the AlAs barrier being positively biased with respect to the superlattice. A clear branching of the peaks due to Stark-ladder formation is observed, as in the ordinary superlattice without an internal surface.⁴ Those branches related to heavy-hole transitions are marked 0, ± 1 , and ± 2 in the negative-polarity region, where 0 is intrawell transition, ± 1 transition between adjacent wells, and ± 2 between the second nearest wells⁴ [see also Figs. 4(a) and 4(b)]. The slopes given by ± 1 and ± 2 transitions agree well (within $\pm 6\%$) with those estimated from V_b/W ,⁷ where W is the total thickness of the undoped region in the structure ($=3240 \text{ \AA}$), and the transitions extrapolate to the middle of the heavy-hole miniband at $V_b = 0 \text{ V}$ as expected. Note that the observation of ± 2 transitions indicates the quantum coherence being at least five periods, or 400 \AA .⁸ In addition to these transitions, there are several novel features, unique to the present structure with an internal surface, marked by *A*, *B*, *C*, and *D*. Region *A* shows an anticrossing between two transitions, one of which originates from the Tamm (HH) transition. A monotonic decrease of the transition energy with increasing electric-field strength is observed at *B*, and new branches are found at *C* and *D*.

In order to understand the features observed in the PC spectra, an EFA calculation has been performed, from which the overlap of electron and hole envelope functions was determined. The overlap is a measure of the one-electron oscillator strength. Figure 4(c) shows the results of the calculation, where dominant transitions are indicated by solid lines as a function of electric field, F . Superimposed are vertical lines indicating the magnitude of the overlaps and the transition energies at a given F . We have used a value of 1.519 eV for the GaAs band gap and ignored excitonic corrections. The horizontal axis is scaled to make possible a direct comparison with Fig. 3, i.e., $F \times W$ gives V_b at the same point of the horizontal axis in Fig. 3.

The anticrossing in region *A* of Fig. 3 is clearly reproduced in Fig. 4(c), where, for clarity, only strong anticrossings are shown by solid lines. The anticrossing is a result of the interaction between the electron Tamm state and the miniband states which undergo Stark localization. A slight increase of the Tamm transition energy arises from the increase in confinement. When the structure is positively biased, the electron Tamm state is lowered with respect to other Stark-localized states. Since there is interwell coupling, whenever the Tamm state crosses a Stark-localized state, anticrossing occurs. The electric fields at which the Tamm state and the state in the $(n+1)$ th well from the internal surface anticross is given by $F = (E_T - E_n)/nD$, where E_T and E_n are the eigenenergy of the Tamm state and the n th lowest-energy state at $F=0$, and D is the period of the superlattice ($=80 \text{ \AA}$).

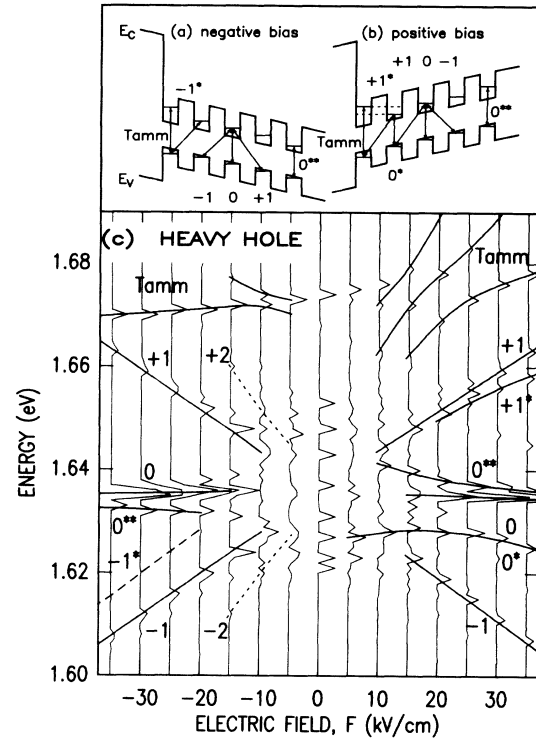


FIG. 4. (a), (b) Schematic diagrams of superlattices under an electric field of 35 kV/cm with transitions corresponding to those indicated in (c). (c) Calculated heavy-hole-related transition energies vs electric field. Also shown as vertical lines is the amount of overlap between electron and heavy-hole envelope functions at corresponding F . Solid lines indicate the major transitions. The dashed line shows a transition observed experimentally but has a small calculated overlap. Dotted lines are ± 2 transitions seen in experiment. Transitions 0^{**} , due to the presence of the other end (AlGaAs side), and $+1^*$ have not been observed in experiment.

The voltage for the anticrossing in Fig. 3 corresponds to an electric field of 20 kV/cm , which, together with the shape of the anticrossing, compares favorably with the one at 25 kV/cm in Fig. 4(c), between the Tamm state and the state localized in the third well from the internal surface. The situation at 35 kV/cm , right after the anticrossing at 25 kV/cm , is illustrated schematically in Fig. 4(b), where the Tamm transition is indicated together with other transitions. When F is increased further in Fig. 4(b), the lowest electron state and the Tamm state undergo the last anticrossing. In the opposite polarity, anticrossing between hole states occurs. Since the heavy-hole miniband is narrower and the separation from the Tamm state smaller, all the anticrossings take place at $F < 5 \text{ kV/cm}$ except for the one shown in the upper left of Fig. 4(c).

In region *B* of Fig. 3, we see a steady decrease in the energy of the transition with increasing F , which parallels the behavior of the Tamm transition in the same region of Fig. 4(c). The reduction of the calculated transition energy is due to the delocalization of the electron

Tamm state with increasing F , caused by a decrease in confinement. We assign transition B of Fig. 3 to the Tamm transition since no light-hole-related structure is expected in this region of the spectrum. Neither can it be accounted for by the transition between excited heavy-hole states, which have extremely small overlap with electrons. This leaves unanswered the question of why the extrapolation of B to 0 V does not give the energy of Tamm transition seen in PLE. The presence of light-hole-related transition near 0 V makes it difficult to track the field dependence of the Tamm transitions, although the possibility exists of these transitions actually being the Tamm transition.

The transition in region C of Fig. 3, also clearly seen in Fig. 4(c) as 0^* , is another result of having an internal surface; its origin is schematically shown in Fig. 4(b). The lowest electron state in Fig. 4(b) has its maximum probability in the second well from the internal surface. When this state undergoes anticrossing, it becomes the Tamm state localized in the left-most well, which means that the transition labeled 0^* becomes -1 , involving the electron Tamm state and the heavy-hole state in the second well. This is the reason for the downward shift of the transition energy seen at $F > 20$ kV/cm. The transition $+1^*$ becomes the Tamm transition after the last anticrossing, which is not resolved experimentally.

The feature in region D of Fig. 3 seems to correspond to transition -1^* of Fig. 4(c), caused once more by the presence of the internal surface and shown in Fig. 4(a). It is not clear why this transition, with relatively small overlap, is seen in the experiment.

Finally, let us briefly mention about the origin of Tamm states from a tight-binding point of view. One can conceptually create a miniband by turning on an interwell coupling in a series of isolated quantum wells. The well at the internal surface has a higher barrier and thus its eigenenergy is higher than those of the rest of the wells. When the coupling is turned on, all the states start to form a miniband except the one at the end because of its high energy; it remains localized and becomes a Tamm state. Alternatively a localized state with an eigenenergy lower than that of the miniband can exist if the barriers in the superlattice are higher than that of the internal surface. Indeed, we have observed this "low-energy" Tamm state in heterostructures with an AlGaAs terminating layer with lower Al content than in the superlattice barriers. In addition to the peaks associated to superlattice interband transitions, PL and PLE spectra revealed a new low-energy feature whose energy and electric-field dependence agreed with the calculated behavior for a low-energy Tamm state. Details of these results are deferred to a future publication.

In summary, we have shown through optical measurements that the introduction of an internal barrier to simulate a surface in superlattices creates localized elec-

tronic states at the internal surface. The positions of the transitions at zero bias as well as their behavior under Stark localization, including anticrossing of the levels, are shown to be in good agreement with the calculation by the envelope-function approximation. We believe, in light of the advancement of fabrication technology of mesoscopic systems, the simulation of various surfaces in a controlled manner in semiconductors will be a powerful tool for studying surface-related phenomena.

We thank Alex Harwit for help in experiments and M. Christie for technical assistance. One of us (H.O.) thanks G. Bastard for useful discussions. This work has been supported in part by the U.S. Army Research Office.

(a)Permanent address: Department of Electrical Engineering, Hokkaido University, Sapporo 060, Japan.

(b)Present address: Instituto de Física, Universidade de Campinas, and Laboratório Nacional de Luz Síncrotron, 13082-Campinas, São Paulo, Brazil.

(c)Present address: Instituto de Ciencia de Materiales (CSIC), Universidad Autónoma, Cantoblanco, E-28049 Madrid, Spain.

¹I. Tamm, Phys. Z. Sowjetunion **1**, 733 (1932).

²C. Pirri, G. Gewinner, J. C. Peruchetti, and D. Bolmont, Phys. Rev. B **38**, 1512 (1988).

³We use the term "Tamm state" to distinguish it from the surface states that appear only after the bands are crossed, e.g., s and p bands in sp^3 bonds, which was first discussed by Shockley [W. Shockley, Phys. Rev. **56**, 317 (1939)]. It is not possible to have Shockley-type surface states in the one-dimensional Kronig-Penney-type potential of the present work.

⁴E. E. Mendez, F. Agulló-Rueda, and J. M. Hong, Phys. Rev. Lett. **60**, 2426 (1988).

⁵The parameters used in the calculation are the following: electron effective mass, $m_e^*/m_0=0.067+0.083x$; heavy-hole effective mass, $m_{HH}^*/m_0=0.340+0.069x$; light-hole effective mass, $m_{LH}/m_0=0.094+0.056x$; conduction-band discontinuity, $\Delta E_C=944x$ (meV); and valence-band discontinuity, $\Delta E_V=550x$ (meV), where m_0 is the free-electron mass and x is the AlAs mole fraction in AlGaAs.

⁶E. S. Koteles and J. Y. Chi, Phys. Rev. B **37**, 6332 (1988). We have assumed that the binding energy of the exciton does not depend significantly on changes in the barrier height, which is a reasonable assumption as long as they are not too large.

⁷The electric field is higher than expected under positive bias. Because of the small barrier of GaAs/Al_{0.2}Ga_{0.8}As against electron injection between the buffer layer and the first superlattice structure, accumulation of electrons at the first AlAs interface occurs, which gives rise to a higher electric field than expected in the remainder of the superlattice structure. Note that the superlattice structure was repeated 3 times. When the bias is negative, the first AlAs from the surface prevents electron injection, assuring the uniformity of the electric field.

⁸F. Agulló-Rueda, E. E. Mendez, and J. M. Hong, Phys. Rev. B **40**, 1357 (1989).